The Nelson Mandela African Institution of Science and Technology

http://dspace.nm-aist.ac.tz

Computational and Communication Science Engineering   Research Articles [CoCSE]

2020-09-24

Two-Factor Authentication Scheme for Mobile Money: A Review of Threat Models and Countermeasures

Ali, Guma

Constant envelope FrFT OFDM: Spectral and energy efficiency analysis

5 authors, including:

Mussa Dida
The Nelson Mandela African Institute of Science and Technology
31 PUBLICATIONS   **31** CITATIONS

Didar Urynbassarova
Beijing Institute of Technology
5 PUBLICATIONS   **21** CITATIONS

Some of the authors of this publication are also working on these related projects:

Project   Educational MS View project

Project   IK and ICTs View project

Constant envelope FrFT OFDM: spectral and energy efficiency analysis

DIDA Mussa Ally[1,2], HUAN Hao[1], TAO Ran[1], WANG Teng[1], and URYNBASSAROVA Didar[1,*]

1. School of Information and Electronics, Beijing Institute of Technology, Beijing 100081, China;
2. School of Computational and Communication Science and Engineering, Nelson Mandela African Institute of Science and Technology, Arusha 23000, Tanzania

Abstract: Constant envelope with a fractional Fourier transform-orthogonal frequency division multiplexing (CE-FrFT-OFDM) is a special case of a constant envelope OFDM (CE-OFDM), both being energy efficient wireless communication techniques with a 0 dB peak to average power ratio (PAPR). However, with the proper selection of fractional order, the first technique has a high bit error rate (BER) performance in the frequency-time selective channels. This paper performs further analysis of CE-FrFT-OFDM by examining its spectral efficiency (SE) and energy efficiency (EE) and compare to the famous OFDM and FrFT-OFDM techniques. Analytical and comprehensive simulations conducted show that, the CE-FrFT-OFDM has five times the EE of OFDM and FrFT-OFDM systems with a slightly less SE. Increasing CE-FrFT-OFDM's transmission power by increasing its amplitude to 1.7 increases its SE to match that of the OFDM and FrFT-OFDM systems while slightly reducing its EE by 20% to be four times that of OFDM and FrFT-OFDM systems. OFDM and FrFT-OFDM's amplitude fluctuations cause rapid changing output back-off (OBO) power requirements and further reduce power amplifier (PA) efficiency while CE-FrFT-OFDM stable operational linear range makes it a better candidate and outperforms the other techniques when their OBO exceeds 1.7. Higher EE and low BER in time-frequency selective channel are attracting features for CE-FrFT-OFDM deployment in mobile devices.

Keywords: fractional Fourier transform (FrFT), constant envelope, spectral efficiency (SE), energy efficiency (EE), high power amplifier.

1. Introduction

Orthogonal frequency division multiplexing (OFDM) is a famous physical layer transmission technique with a high data rate and ease of implementation using fast Fourier transform (FFT). The main drawback of the OFDM modulated waveform is high amplitude fluctuations that

produce large peak to average power ratio (PAPR). The high PAPR makes the OFDM sensitive to nonlinear distortion and high energy requirement for wireless communicating handheld devices [1].

This and other drawbacks such as its sensitiveness to carrier frequency offset make the OFDM unfit for the next generation mobile device usage. Different techniques were applied to reducing or eliminating OFDM PAPR drawbacks as discussed in [2,3], which are mainly categorized as signal scrambling techniques and signal distortion techniques.

The 0 dB PAPR signal scrambling techniques include a constant envelope OFDM (CE-OFDM) presented in [4] and a CE fractional Fourier transform OFDM (CE-FrFT-OFDM) or simply named CE chirped OFDM discussed in our earlier research in [5]. The techniques attain the same symbol error rate (SER) as the conventional OFDM and the FrFT-OFDM with ease of deployment and 100% amplifier efficiency in its operation. The CE-FrFT-OFDM uses the advantages of FrFT as discussed in [6] and [7] to implement CE-OFDM as developed by [4] and its symbol error rate (SER) performance was analyzed in [8].

The advantages of the CE-FrFT-OFDM includes high SER as conventional OFDM, high power amplifier (PA) energy efficiency, additional system security due to the signal spreading which creates a noise-like waveform suitable for secure and low probability of intercept (LPI) communications as in [9]. Unlike the CE-FrFT-OFDM proposed in [10] and its performance analyzed in [11], which has limited range of applications as it only uses Barker codes, the CE-FrFT-OFDM in [5,8] has a wide range of applications as it uses any modulated signal like M-ary quadrature amplitude modulation (M-QAM), M-ary phase shift keying (M-PSK), and offset quadrature amplitude modulation (OQAM) with a M-PSK coverage in this paper.

However, 0 dB PAPR, 100% PA efficiency, and high

SER are not the only performance conditions needed by a next generation communication system. Other conditions include system complexity for system feasibility, spectrum efficiency (SE) and energy efficiency (EE) for efficient use of available bandwidth and energy as discussed in [12]. Since the CE-FrFT-OFDM uses FrFT in its operation with the same complexity and power consumption as FFT in a traditional OFDM [13], then, the CE-FrFT-OFDM has the same complexity and power consumption as the conventional OFDM with the exception of signal extension and its wrapping into CE. The fact that the additional operations in the CE-FrFT-OFDM are in the real-valued signal reduces extra memory requirement and power consumptions [14]. It is an added advantage and the increasing need of its further exploration.

The main objective of this paper is to further discuss the CE-FrFT-OFDM by analytically finding its SE and EE, compare the analytical results with simulations, the traditional OFDM and the FrFT-OFDM systems. The rest of the paper is organized as follows. Section 2 gives the review of the CE-FrFT-OFDM. Section 3 gives SE and EE analytical calculations of the system. Section 4 gives the detailed SE and EE system simulations and comparison to the OFDM and the FrFT-OFDM. Lastly, Section 5 concludes the paper and provides recommendations for future work on CE-FrFT-OFDM systems.

2. System model

This section provides a review of a CE-FrFT-OFDM signal generation as depicted by a block diagram in Fig. 1. The main stages of CE-FrFT-OFDM formation is obtaining a time-domain signal by using an inverse FrFT (IFrFT) as given by

$$s_i(m) = \sum_{k=0}^{N-1} S_i(k) F_{-\alpha}(m,k), \quad 0 \leqslant m < N-1 \quad (1)$$

where $S_i(k)$ is the modulated signal (PSK is used in this paper), $F_{-\alpha}(m,k)$ is the IFrFT transform as detailed explained in [15,16]. The FrFT is given by

$$F_\alpha(m,n) = \sqrt{\frac{\sin\alpha - j \cdot \cos\alpha}{N}} \exp\left(\frac{j}{2} m^2 \cot\alpha(u)^2\right) \times$$

$$\exp\left(\frac{j}{2} n^2 \cot\alpha(T_s^2)\right) \exp\left(-j\frac{2\pi mn}{N}\right) \quad (2)$$

where $\alpha = p \cdot \frac{\pi}{2}$ $(0 < \alpha < \pi)$, p is the fractional factor of the transform, Δu is the sampling space in the fractional Fourier domain, and $\Delta u T_s = \frac{2\pi|\sin\alpha|}{N}$. When $\alpha = \frac{\pi}{2}$, the system becomes a traditional OFDM system (FFT-OFDM) and the obtained system will be CE-OFDM.
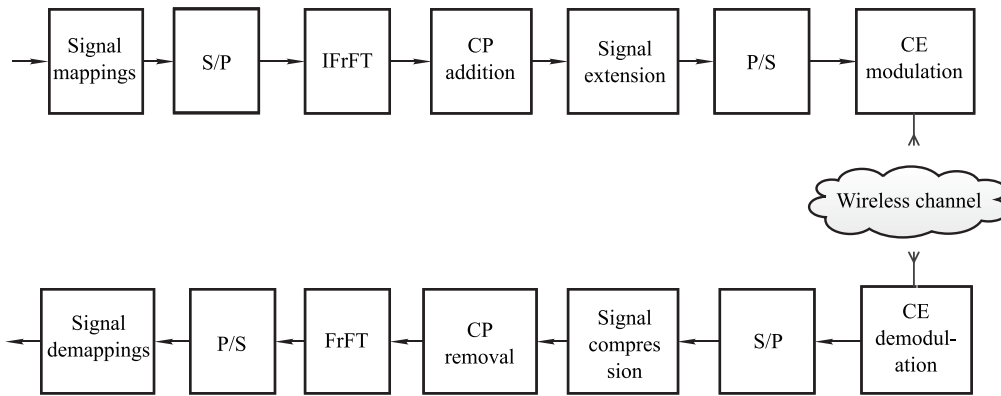

Fig. 1   CE-FrFT-OFDM block diagram

Then, to get a CE-FrFT-OFDM, the obtained time-domain signal $s_i(m)$ is extended to obtain a real-valued time signal as shown by (3) and wrapped by a CE waveform as given by (4).

$$m_i = \begin{bmatrix} I_{N\times N} \\ 0_{N\times N} \end{bmatrix} \Re(s_i)^H + \begin{bmatrix} 0_{N\times N} \\ I_{N\times N} \end{bmatrix} \Im(s_i)^H \quad (3)$$

where $(\cdot)^H$ represents the transpose operation, $I_{N\times N}$ is an $N \times N$ identity matrix, $0_{N\times N}$ is an $N \times N$ zero matrix and $\Re(\cdot)$ and $\Im(\cdot)$ stand for real and imaginary operations.

Signal extension operation creates a noise-like waveform which is suitable for increasing security of the communicating devices as discussed in [9]. Cyclic prefix (CP) can be added as a guide band to eliminate inter-symbol interference (ISI) of the transmitted information but for simplicity CP overhead is not covered in this paper. Then, the CE of the real-valued signal generated is obtained by phase modulating the signal m_i as given by

$$x_i = A\exp(j(2\pi h_{\mod} \cdot m_i + \theta_i)) \quad (4)$$

where $h_{\mod}$ is a constant modulation index (MI), $j = \sqrt{-1}$, and θ_i is the ith subcarrier angle for increasing chan-

nel estimation efficiency given by $\theta_i = \theta_{i-1} + 2\pi\dfrac{i}{N}$ with $\theta_0 = 0$.

The signal is then amplified and transmitted through a wireless channel. The received signal is the results of wireless channel impulse response (CIR) and additive white Gaussian noise (AWGN) as given by (5). The receiver executes inverse operations in reverse order to estimate the transmitted signal.

$$y_i = h_i \otimes x_i + w_i \tag{5}$$

where h is CIR, $\otimes$ is convolution operation, x is the transmitted signal and w is the noise between the transmitter and receiver. In the frequency domain, it can be easily represented by $\boldsymbol{Y} = \boldsymbol{HX} + \boldsymbol{W}$.

In implementations, $N = 64$ FrFT size is used followed by signal extension to obtain $2N$ phased modulated subcarriers. The implementations need additional computation/circuit for signal extension and wrapping with additional 10% to 15% circuit power consumption requirement as stated in [17,18]. However, PAPR elimination will further reduce 40% of the amplification power [19] and therefore gives the overall best system power consumption than OFDM and FrFT-OFDM systems.

3. SE and EE analysis

3.1 SE

SE is a widely accepted criterion for wireless network optimization. It measures the system throughput per given bandwidth. According to Shannon's formula [20], the achievable data rate over an AWGN channel could be expressed by

$$C = B \log_2(1 + \text{SNR}) = B \log_2\left(1 + \frac{P_y}{P_w}\right) \tag{6}$$

where B is the bandwidth, SNR is the signal to noise ratio, P_y is the average received power, and P_w is the AWGN average power.

Due to receivers estimation errors, the signal to noise ratio is further decreased by incresed signal distortions caused by estimation errors and the overall channel throughput is given by

$$C = B \log_2(1 + \text{SNDR}) = B \log_2\left(1 + \frac{P_y}{P_d + P_w}\right) \tag{7}$$

where SNDR is the signal to noise distortion ratio, and P_d is the power of the nonlinear distortion noise.

For a multicarrier systems in a multipath wireless communication channel, its capacity is given by (7) as detailed

explained in [21–23]. By using (7) we obtain the CE-FrFT-OFDM system capacity given by

$$C = B \sum_{i=1}^{N} \log_2\left(1 + \frac{\dfrac{1}{L}\displaystyle\sum_{l=0}^{L-1}|H(W^l)|^2 P_i}{\sigma_\Delta^2 P_i + \sigma_w^2}\right) \tag{8}$$

where N is the number of subcarriers, L is the multipath taps, $H(W^l)$ is the channel impulse response in the frequency domain for the first path, and P_i is power for the ith subcarrier given by $P_i = \displaystyle\int_{-\frac{T}{2}}^{\frac{T}{2}} x_i(t) \cdot x_i(t)^* \mathrm{d}t$ with $(\cdot)^*$ being the complex conjugate, and σ_Δ^2 is the minimum mean square error (MMSE) variance due to equalization and σ_w^2 is the AWGN variance.

$$C_{\text{CE-FrFT-OFDM}} = \frac{1}{2}B \log_2\left(1 + \frac{\text{E}[|H(W^l)|^2]P_x}{\sigma_\Delta^2 P_x + \sigma_w^2}\right) \tag{9}$$

where $\text{E}[\cdot]$ is the expectation operation, and P_x is the average transmit power of the CE-FrFT-OFDM subcarrier.

By using block type pilot symbols, the receiver is assumed to have partial channel state information (CSI) and can be used to determine the CIR of the Rayleigh fading channel which is a good model for analyzing performance of the CE-FrFT-OFDM in indoor environments.

A least square (LS) estimator or MMSE estimator can be used to approximate and equalize the transmitted signal with an alternative of the training sequence. The CIR obtained by LS and MMSE estimators is given by

$$\overline{H}_{\text{LS}} = X_P^{-1} Y_P \tag{10}$$

$$\overline{H}_{\text{MMSE}} = R_{\text{HH}}(R_{\text{HH}} + \sigma_n^2(X_P X_P^H)^{-1})^{-1}\overline{H}_{\text{LS}} \tag{11}$$

where $\overline{H}$ is the estimated complex-value Rayleigh fading random variable (CIR) in the frequency domain $\overline{H} = [\overline{H}_0, \overline{H}_1, \ldots, \overline{H}_{L-1}]$, X_P and Y_P are transmitted and received pilot symbols respectively and R_{HH} is channel autocorrelation.

Although the OFDM, the FrFT-OFDM, and the CE-FrFT-OFDM pass through the same wireless channel, each one will be affected differently as each has different peak values and fluctuations. The CE-FrFT-OFDM, the FrFT-OFDM, and the OFDM channel responses are shown in Fig. 2. The CIRs are of equal nature and determined by the type of channel intead of the waveform type but the SE and EE will vary depending on the signal strength of each waveform as shown in Fig. 3 and Fig. 4.
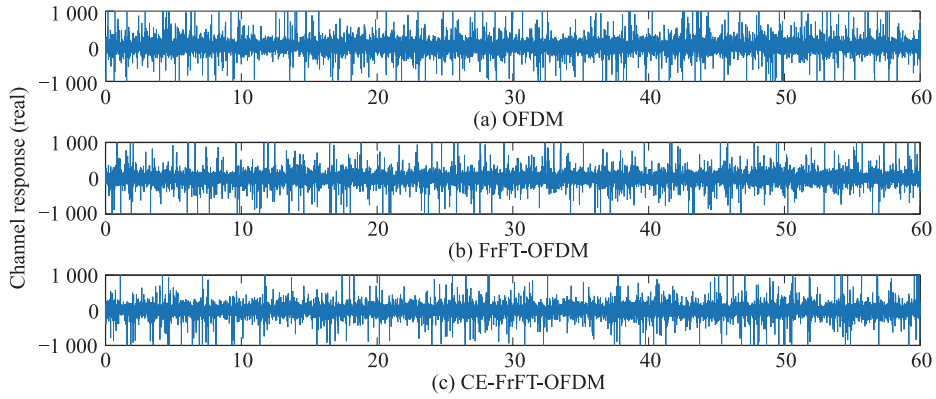
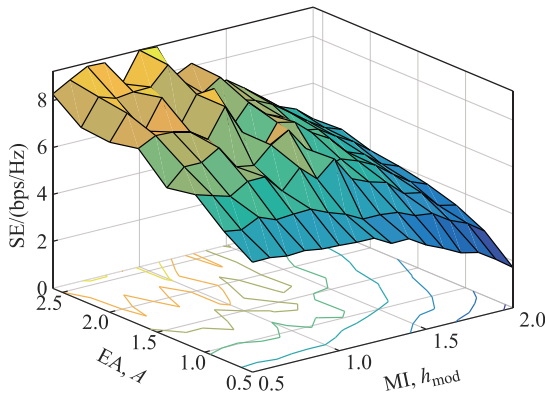**Fig. 2   OFDM, FrFT-OFDM, and CE-FrFT-OFDM channel impulse responses**

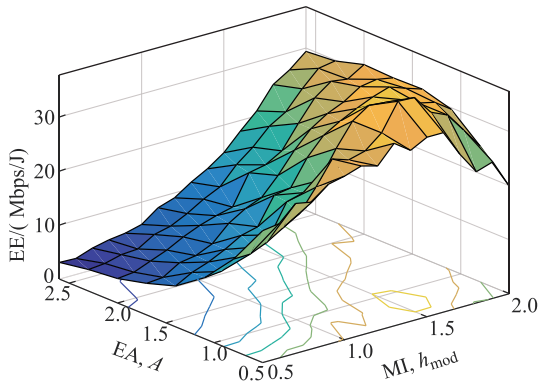**Fig. 3   SE of CE-FrFT-OFDM against MI and amplitude when SNR=15 dB**

Fig. 4   EE of CE-FrFT-OFDM against MI and amplitude when SNR=15 dB

The overall CE-FrFT-OFDM SE is given by

$$\eta_{\text{SE}} = \frac{1}{2} \log_2 \left(1 + \frac{\text{E}[|H(W)|^2]P_x}{\sigma_\Delta^2 P_x + \sigma_w^2} \right). \tag{12}$$

Compared with OFDM, the ratio between the CE-FrFT-

OFDM and OFDM SE is given by

$$\frac{\eta_{\text{SE}_1}}{\eta_{\text{SE}_2}} = \frac{\frac{1}{2} \log_2 \left(1 + \frac{\text{E}[H_1]^2 P_1}{\sigma_\Delta^2 P_1 + \sigma_w^2} \right)}{\log_2 \left(1 + \frac{\text{E}[H_2]^2 P_2}{\sigma_\Delta^2 P_2 + \sigma_w^2} \right)}. \tag{13}$$

Simplify (13) and we obtain

$$\frac{\eta_{\text{SE}_1}}{\eta_{\text{SE}_2}} = \frac{\frac{1}{2} \log_2 \left(\dfrac{\sigma_\Delta^2 + \dfrac{\sigma_w^2}{P_1} + \text{E}[H_1]^2}{\sigma_\Delta^2 + \dfrac{\sigma_w^2}{P_1}} \right)}{\log_2 \left(\dfrac{\sigma_\Delta^2 + \dfrac{\sigma_w^2}{P_2} + \text{E}[H_2]^2}{\sigma_\Delta^2 + \dfrac{\sigma_w^2}{P_2}} \right)}. \tag{14}$$

Thus, under the same transmit power, i.e., when $P_1 = P_2$, and the same noise energy, i.e., $\text{E}[H_1]^2 = \text{E}[H_2]^2$, $\eta_{\text{SE}_1} = \dfrac{\eta_{\text{SE}_2}}{2}$, but increasing P_1 also increases η_{SE_1} to match η_{SE_2} as shown in Fig. 3.

3.2   EE

In addition to throughput improvement, EE is becoming an increasingly important factor for mobile communications because of the slow progress of battery technology. EE defines the amount of energy used by a communication system to transmit the given information [24,25]. EE is simply defined as the system throughput divided by the total system power consumption.

Moreover, the mobile devices also incur additional circuit power during transmissions. The circuit power represents the average energy consumption of device electronics, such as mixers, filters, and digital-to-analogy converters. In a transmit mode, the EE of the CE-FrFT-OFDM is given by

$$\eta_{\text{EE}} = \frac{C_{\text{CE-FrFT-OFDM}}}{P_T} = \frac{C_{\text{CE-FrFT-OFDM}}}{\kappa P_x + P_C} =$$

$$\frac{B}{2(\kappa P_x + P_C)} \log_2 \left(1 + \frac{\mathrm{E}[|H(W)|^2]P_x}{\sigma_\Delta^2 P_x + \sigma_w^2} \right) \qquad (15)$$

where κ is a constant depending on the amplifier operational efficiency, P_x is the transmit signal power and P_C is the circuitry power consumptions.

For the CE-FrFT-OFDM, $\kappa = 1$. Since it has 100% power amplification efficiency but $\kappa \geqslant 3$ for OFDM and FrFT-OFDM as they attain maximum amplifier efficiency of 30%.

Take EE of the CE-FrFT-OFDM as $\eta_{\mathrm{EE}_1} = \dfrac{C_1}{\kappa_1 P_1 + P_c}$, and EE of OFDM as $\eta_{\mathrm{EE}_2} = \dfrac{C_2}{\kappa_2 P_2 + P_c}$.

Compare the two EEs:

$$\frac{\eta_{\mathrm{EE}_1}}{\eta_{\mathrm{EE}_2}} = \frac{C_1}{\kappa_1 P_1 + P_c} \cdot \frac{\kappa_2 P_2 + P_c}{C_2}. \qquad (16)$$

For the same channel capacity, i.e., $C_1 = C_2$, and from $\kappa_1 = 1$ and $\kappa_2 \geqslant 3$, we get

$$\frac{\eta_{\mathrm{EE}_1}}{\eta_{\mathrm{EE}_2}} = \frac{\kappa_2 P_2 + P_c}{P_1 + P_c}. \qquad (17)$$

So for the same transmission power, i.e., $P_1 = P_2$, the CE-FrFT-OFDM will have better EE than OFDM, i.e., $\eta_{\mathrm{EE}_1} > \eta_{\mathrm{EE}_2}$, as it is proved in Fig. 4.

3.3 Transmission under power amplifier

Under PA, the signal power P_x is amplified with the gain g, and to reduce energy consumption signal clipping is employed when $P_{\mathrm{in}} \geqslant P_{\mathrm{in}}^{\mathrm{max}}$ as given by

$$P_{\mathrm{out}} = \begin{cases} gP_{\mathrm{in}}, & P_{\mathrm{in}} < P_{\mathrm{in}}^{\mathrm{max}} \\ gP_{\mathrm{in}}^{\mathrm{max}}, & P_{\mathrm{in}} \geqslant P_{\mathrm{in}}^{\mathrm{max}} \end{cases} \qquad (18)$$

where P_{out} is the amplifier output signal power, $P_{\mathrm{in}} = P_x$ is the signal power, $g \geqslant 1$ is the amplifier gain and $P_{\mathrm{in}}^{\mathrm{max}}$ is a maximum signal power which causes amplifier saturation.

Unlike multicarrier systems, the CE-FrFT-OFDM has a high linear range of operation and has a 0 dB PAPR. In multicarrier systems power back-off factor is used to increase the operational linear range of an amplifier. The input back-off (IBO) and output back-off (OBO) further increases SNDR hence reducing system capacity as given in [19]. The SNDR in a multicarrier system is given by

$$\mathrm{SNDR} = \frac{1}{\mathrm{OBO}} \left(\frac{P_y}{P_d + P_w} \right) \qquad (19)$$

where $\mathrm{OBO} = \dfrac{P_{\mathrm{out}}^{\mathrm{max}}}{P_{\mathrm{in}}^{\mathrm{avg}}}$.

In multicarrier systems, $\mathrm{OBO} > 1$, which increases signal distortion and makes $\mathrm{SNDR}_{\mathrm{MC}} <$

$\mathrm{SNDR}_{\mathrm{CE\text{-}FrFT\text{-}OFDM}}$, and hence SE and EE of the CE-FRFT-OFDM are always greater than those of the OFDM and the FrFT-OFDM systems as shown in Fig. 5.
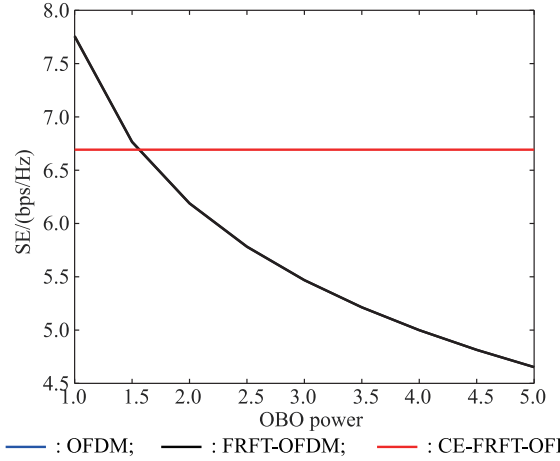

Fig. 5 SE comparisons for CE-FrFT-OFDM, OFDM and FrFT-OFDM under HPA when $\mathrm{SNR} = 15$

4. Simulation results

The parameters used in the simulation are tabulated in Table 1.

Table 1 System parameters

SN	Information	Value
1	Subcarrier size	64
2	Guard band	8
3	Modulation type	8-PSK
4	Fractional order	0.1
5	Number of symbols	10 000
6	MI h_{mod}	1
7	Envelope amplitude (EA)	1.5
8	Doppler frequency/Hz	100
9	Signal delay/μs	1,10
10	Delayed signal power/dB	$-4, -2$
11	Subcarrier bandwidth/MHz	2
12	Maximum transmit power/W	3
13	Circuit power/W	0.2
14	Amplifier gain/g	1

In analyzing the SE and EE of the CE-FrFT-OFDM, we compute their values under different MI and EA as shown in Fig. 3 and Fig. 4. The first shows that an increase of MI reduces SE but the increase of EA increases SE of the system. The latter shows an increase of MI leads to the increase of EE while increasing EA reduces EE. Bases on this, the trade-off between EE and SE has to be made for the best system operation condition. Since the CE-FrFT-OFDM is an energy efficient system, we compromise EE for better SE and the preferred choice for EA and MI is 1.5 and 1 respectively as tabulated in Table 1.

The selected MI and EA are used to find SE and EE of the system and compare to OFDM and FrFT-OFDM systems as shown in Fig. 6 and Fig. 7. The first shows that,

the SE of the CE-FrFT-OFDM is slightly less than that of the OFDM and the FrFT-OFDM but it can be increased to match other systems by increasing its EA from 1.5 to 1.7 as shown by Fig. 3 and Fig. 4.
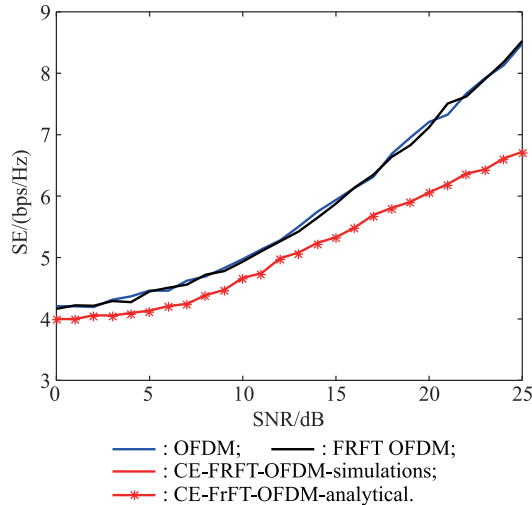

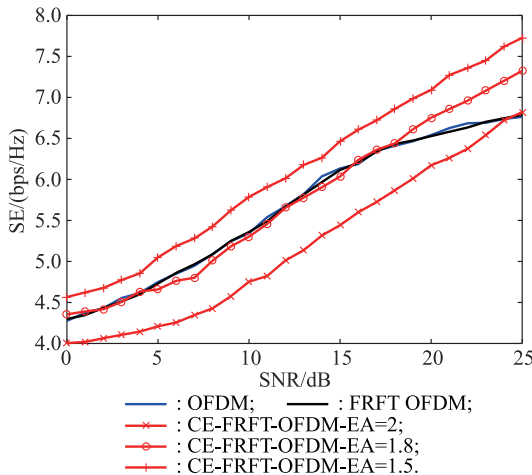**Fig. 6   SE for CE-FrFT-OFDM and its comparison to OFDM and FrFT OFDM**

Fig. 7   SE of CE-FrFT-OFDM under different EA

Fig. 7 shows the EE of the system is five times that of OFDM and FrFT-OFDM. In increasing EA of the CE-FrFT-OFDM system we increase SE to match shows that the SE of CE-FrFT-OFDM is constant while the SEs of OFDM and FrFT-OFDM decrease or exceed that of OFDM and FrFT-OFDM systems. Fig. 6 further compares SE of the systems under high PA with different OBO. It is abruptly when increasing OBO and it is outperformed by CE-FrFT-OFDM when OBO is greater than 1.7.

5. Conclusions

In this paper, we discuss the implementation of the CE-FrFT-OFDM. The SE and EE of the CE-FrFT-OFDM are analyzed to show the effectiveness of the system. Fig. 3 and Fig. 4 show how the optimized waveform amplitude and MI are obtained in our system. Using the optimized value, the SE and EE of the system are found and analyzed under different SNR, and compared to OFDM and FrFT-OFDM systems as shown in Fig. 6 and Fig. 7.

The simulation proves the CE-FRFT-OFDM is a energy efficient system with slightly less SE. Fig. 6 shows the SE of the system can easily match that of the OFDM and the FrFT-OFDM when amplitude of the waveform is increased. Fig. 5 shows the system has better performance than the OFDM and the FrFT-OFDM when operated under amplifier with an OBO of at least 1.7.

The high SE and EE proved here plus the same SER performance as the OFDM and the FrFT-OFDM show in our previous research proves that the CE-FrFT-OFDM is a good waveform of choice for use in wireless communication devices.

Acknowledgment

References

[1]   CHIUEH T D, TSAI P Y. OFDM baseband receiver design for wireless communications. Singapore: John Wiley and Sons (Asia).

[2]   JIANG T, WU Y. An overview: peak-to-average power ratio reduction techniques for OFDM signals. IEEE Trans. on Broadcasting, 2008, 54(2): 257 – 268.

[3]   HAN S H. An overview of peak-to-average power ratio reduction techniques for multicarrier transmission. IEEE Wireless Communication, 2005, 12(2): 56 – 65.

[4]   THOMPSON S C, AHMED A U, PROAKIS J G, et al. Constant envelope OFDM. IEEE Trans. on Communications, 2008, 56(8): 1300 – 1312.

[5]   DIDA M A, HAO H, WANG X, et al. Constant envelope chirped OFDM for power-efficient radar communication. Proc. of the Information Technology, Networking, Electronic & Automation Control Conference, 2016: 298 – 301.

[6]   MARTONE M. A multicarrier system based on the fractional Fourier transform for time-frequency-selective channels. IEEE Trans. on Communications, 2001, 49(6): 1011 – 1020.

[7]   TAO R, DENG B, WANG Y. Research progress of the fractional Fourier transform in signal processing. Science in China Series F Information Sciences, 2006, 49(1): 1 – 25.

[8]   DIDA M A, HAO H, ANJUM M R, et al. Constant envelope chirped OFDM power efficiency. Proc. of the 4th International Conference on Wireless and Optical Communications, 2016: 99020N.

[9]   DIDA M A, HAO H, WANG T, et al. Constant envelope FrFT-OFDM with physical layer security. Proc. of the 7th International Workshop on Computer Science and Engineering, 2017: 794 – 799.

[10] ILIOUDIS C V, CLEMENTE C, PROUDLER I, et al. Constant envelope fractional fourier transform based waveform libraries for MIMO radar. Proc. of the Sensor Signal Processing for Defence, 2014: 1–5.

[11] ILIOUDIS C V, CLEMENTE C, PROUDLER I, et al. Performance analysis of fractional waveform libraries in MIMO radar scenario. Proc. of the Radar Conference, 2015: 1119–1124.

[12] SAXENA R, SINGH A K, JOSHI H D, et al. Exact BER analysis of FRFT-OFDM system over frequency selective Rayleigh fading channel with CFO. Electronics Letters, 2013, 49(20): 1299–1301.

[13] BENALI W, BOT M L, LANGLAIS C, et al. Power consumption of Wi-Fi transceivers. Proc. of the International Symposium on Wireless Communication Systems, 2016: 213–217.

[14] HSUE W L, CHANG W C. Real discrete fractional fourier, hartley, generalized fourier and generalized hartley transforms with many parameters. IEEE Trans. on Circuits and Systems I: Regular Papers, 2015, 62(10): 2594–2605.

[15] OZAKTAS H M, ARIKAN O, KUTAY M A, et al. Digital computation of the fractional Fourier transform. IEEE Trans. on Signal Processing, 1996, 44(9): 2141–2150.

[16] PEI S C, YEH M H. The discrete fractional cosine and sine transforms. IEEE Trans. on Signal Processing, 2001, 49(6): 1198–1207.

[17] QIAN Z, MARGALA M. Low-power split-radix FFT processors using Radix-2 butterfly units. IEEE Trans. on Very Large Scale Integration Systems, 2016, 24(9): 1–5.

[18] BROKALAKIS A, PALIOURAS V. Using the arithmetic representation properties of data to reduce the area and power consumption of FFT circuits for wireless OFDM systems. Proc. of the Signal Processing Systems, 2011: 7–12.

[19] JIANG T, LI C, NI C. Effect of PAPR reduction on spectrum and energy efficiencies in OFDM systems with Class-A HPA over AWGN channel. IEEE Trans. on Broadcasting, 2013, 59(3): 513–519.

[20] SHANNON C E. Communication in the presence of noise. Proceedings of the IRE, 2006, 37(1): 10–21.

[21] GOLDSMITH A. Wireless communications. New York, USA: Cambridge University Press, 2005.

[22] THOMAS M C, JOY A T. Elements of information theory. 2nd ed. New York, USA: Wiley, 2006.

[23] AMIN O, BEDEER E, AHMED M H, et al. Energy efficiency and spectral efficiency trade-off for OFDM systems with imperfect channel estimation. Proc. of the IEEE International Conference on Communications, 2014: 3559–3564.

[24] JOUNG J, HO C K, SUN S. Spectral efficiency and energy efficiency of OFDM systems: impact of power amplifiers and countermeasures. IEEE Journal on Selected Areas in Communications, 2014, 32(2): 208–220.

[25] MIAO G, VÄSTBERG A. Energy efficiency in the wideband regime. IEEE Trans. on Wireless Communications, 2013, 12(8): 4102–4109.

Biographies

DIDA Mussa Ally was born in 1983. He received his Ph.D. degree in Information and Communication Engineering from Beijing Institute of Technology in 2017, Ms.c. in Telecommunications Engineering from University of Dodoma in 2011, and B.Sc. in Computer Engineering and Information Technology from University of Dar es Salaam in 2008. Currently he is working as a lecturer at Nelson Mandela African Institute of Science and Technology in Arusha, Tanzania. His research interests are in the field of digital signal processing, fractional fourier signals and systems, single carrier and multicarier systems.
E-mail: mussa.ally@nm-aist.ac.tz
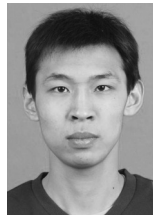
HUAN Hao was born in 1983. He received his B.S. degree from Zhengzhou Univerversity and Ph.D. degree from Beijing Institute of Technology in 2013. In 2016 he was a visiting scholar in the University of Delaware, State of delaware, USA. He is currently a lecturer with the school of Information and Electronics, Beijing Institute of Technology. His research interests include physical layer security for wireless communication, satellite communication, and radar signal processing.
E-mail: huanhao@bit.edu.cn

TAO Ran was born in 1964. He received his B.S. degree from Hefei College of Electronic Engineering, Hefei, in 1985 and the M.S. and Ph.D. degrees from Harbin Institute of Technology, Harbin, in 1990 and 1993, respectively. In 2001, he was a senior visiting scholar in the University of Michigan, Ann Arbor. He is currently a professor with the School of Information and Electronics, Beijing Institute of Technology, Beijing, China. He has been a distinguished professor of Changjiang Scholars Program since 2009 and a chief professor of the Program for Changjiang Scholars and Innovative Research Team in University since 2010. His current research interests include fractional Fourier transform with applications, theory and technology for radar and communication systems.
E-mail: taoran@bit.edu.cn

WANG Teng was born in 1988. He is currently a Ph.D. candidate at the School of Information and Electronics of Beijing Institute of Technology, China. His research interests lie in the field of physical layer security for wireless communication, time-frequency analysis, fractional Fourier transform and satellite communication.
E-mail: wangteng@bit.edu.cn

URYNBASSAROVA Didar was born in 1990. She received her B.Ed. degree in mathematics from Aktobe State Pedagogical Institute, Aktobe, Kazakhzstan, in 2011 and her M.S. degree from the Aktobe State University named after K. Zhubanov, Aktobe, Kazakhstan, in 2013, and Ph.D. degree from Beijing Institute of Technology, Beijing, China, in 2018. Her research interests are in the areas of the Fourier transform, linear canonical transform, time-frequency signal processing, and signal processing for radar and communications.
E-mail: didaruzh@mail.ru